Available online at www.sciencedirect.com

SciVerse ScienceDirect

Ceramics International 38 (2012) 5993–5997

CERAMICS INTERNATIONAL

www.elsevier.com/locate/ceramint

# Dielectric and Magnetic properties of $(1-x)BiFeO_3$–$xBa_{0.8}Sr_{0.2}TiO_3$ ceramics

H. Khelifi [a], M. Zannen [a], N. Abdelmoula [a,*], D. Mezzane [b], A. Maalej [a], H. Khemakhem [a], M. Es-Souni [c]

[a] *Laboratoire des Matériaux Ferroélectriques (LMF), Unité de Physique-Mathématiques 05UR15-04, Université de Sfax, Faculté des Sciences de Sfax (FSS), Route de Soukra km 3.5, B.P. 1171, 3000 Sfax, Tunisia*

[b] *Laboratoire de la Matière Condensée et Nanostructures (LMCN), Université Cadi Ayyad, Faculté des Sciences et Techniques Gueliz (FSTG), B.P. 549, Marrakech, Morocco*

[c] *Institute for Materials and Surface Technology, University of Applied Science of Kiel, Grenzstrasse 3, 24149 Kiel, Germany*

Received 13 January 2012; received in revised form 29 March 2012; accepted 19 April 2012
Available online 27 April 2012

**Abstract**

The polycrystalline samples of $(1-x)BiFeO_3$–$xBa_{0.8}Sr_{0.2}TiO_3$ ($x = 0, 0.1, 0.2, 0.25, 0.3, 0.4$ and $x = 1$) were prepared by the conventional solid state reaction method. The effect of substitution in $BiFeO_3$ by $Ba_{0.8}Sr_{0.2}TiO_3$ on the structural, dielectric and magnetic properties was investigated. X-ray diffraction study showed that these compounds crystallized at room temperature in the rhombohedral distorted perovskite structure for $x \leq 0.3$ and in cubic one for $x = 0.4$. As $Ba_{0.8}Sr_{0.2}TiO_3$ content increases, the dielectric permittivity increases. This work suggests also that the $Ba_{0.8}Sr_{0.2}TiO_3$ substitution can enhance the magnetic response at room temperature. A remanent magnetization $M_r$ and a coercive magnetic field $H_C$ of about 0.971 emu/g and 2.616 kOe, respectively were obtained in specimen with composition $x = 0.1$ at room temperature.


*Keywords:* C. Dielectric properties; C. Magnetic properties; D. Perovskite; Ceramics

## 1. Introduction

Multiferroic materials exhibit ferroelectric and magnetic properties simultaneously within a single phase. These materials are considered to offer potential in novel devices such as multi-state memory devices, transducers and sensors [1,2]. In the conventional mechanism of ferroelectricity in perovskite, an off-centring of B-site cations, requires the B site to have an empty *d* orbital, which is incompatible with magnetic ordering from partially filled *d* shells [3]. Thus, there are very few single phase multiferroic materials in nature. Bismuth ferrite $BiFeO_3$ is one of multiferroic materials [4]. $BiFeO_3$ is ferroelectric below $T_C \approx 830$ °C and G-type antiferromagnetic below $T_N \approx 370$ °C, with cycloidal spin magnetic arrangement [5]. $BiFeO_3$ crystallizes in a rhombohedral structure at room temperature with *R*3*c* space group [6]. The preparation of $BiFeO_3$ in the bulk form without traces of impurities has been a difficult task. Sosnowska et al. [5] observed an impurity peak of $Bi_2Fe_4O_9$ and Tabares-Munoz et al. [7] that of $Bi_{46}Fe_2O_{72}$. Therefore, $BiFeO_3$–$ABO_3$ solid–solution systems such as $PbTiO_3$ [8], $BaTiO_3$ [9–11] and $NaNbO_3$ [12] and $SrTiO_3$ [13], have attracted great attention as a means to increase structural stability. Furthermore, $BiFeO_3$ ceramic is characterized by high leakage, small permittivity, high dielectric losses and multiple thermally activated relaxations in kHz range [14,15].

$Ba_{0.8}Sr_{0.2}TiO_3$ is a prototype ferroelectric material with several excellent ferroelectric properties ($T_C = 75$ °C, and $\varepsilon_r \sim 11{,}500$) [16] better than $BaTiO_3$ ($T_C$: 120 °C, and $\varepsilon_r \sim 9000$) [17], the structure of $Ba_{0.8}Sr_{0.2}TiO_3$ has tetragonal phase at room temperature [16], and is expected that both ferroelectricity and ferromagnetism still coexist in the compound formed when mixed with $BiFeO_3$.

The aim of the present work is to study the structural, dielectric and magnetic properties of the $(1-x)BiFeO_3$–$xBa_{0.8}Sr_{0.2}TiO_3$ ceramics with $x = 0.1$, 0.2, 0.3, 0.4 and 1.

* Corresponding author. Tel.: +216 97 234 510; fax: +216 74 274 437.
*E-mail address:* najmeddine.abdelmoula@fss.rnu.tn (N. Abdelmoula).

0272-8842/$36.00 
http://dx.doi.org/10.1016/j.ceramint.2012.04.055

## 2. Experimental

The $(1-x)BiFeO_3$–$xBa_{0.8}Sr_{0.2}TiO_3$ ($x = 0$, 0.1, 0.2, 0.25, 0.3, 0.4 and $x = 1$) ceramics were prepared using solid state reaction method. For compositions in the range $0 \leq x \leq 0.4$ compositions, high purity $Bi_2O_3$, $Fe_2O_3$, $TiO_2$, $BaCO_3$ and $SrCO_3$ powders were carefully weighed in stoichiometric proportions and thoroughly mixed in agate mortar for 2 h. Bismuth oxide was taken in 5% mole excess to compensate bismuth loss during sintering process. In order to obtain single phase samples, the powders were then pressed into discs and calcined rapidly at 600 °C for 1 h and later at 800 °C for 2 h with intermediate grindings. After calcination, samples were grounded for 2 h and pressed into pellets, then heated at 830 °C for 1 h in air with a high heating rate. For the composition $x = 1$, the appropriate mixture of powder was calcined at 1100 °C for 12 h. After being carefully milled, the powder was then pressed into pellets, and finally sintered at 1320 °C for 3 h.

The crystal structures of the sintered samples were examined by an X-ray diffraction (XRD, XPERT-PRO) with Cu Kα radiation (λ = 1.5406 Å), 0.02° scan step and 1 s/step counting time. The microstructure of the samples was examined by a scanning electron microscopy (Zeiss Ultra plus 40, Germany). The dielectric measurements were studied using LCR meter HP 4284A. The temperature and frequency ranges were between 30 and 600 °C and 100–1000 kHz, respectively. The magnetization hysteresis (*M–H*) loop was performed using vibrating sample magnetometer (NanoMOKE2 of Germany) superconducting quantum interference device (SQUID) at room temperature.

## 3. Results and discussion

### 3.1. Phase purity and microstructures

The X-ray diffraction (XRD) patterns were analyzed to confirm the phase purity, the symmetry and to calculate the lattice parameters for all compositions of the solid solution $(1-x)BiFeO_3$–$xBa_{0.8}Sr_{0.2}TiO_3$. A profile matching of the XRD spectra was made using the ''Fullproof'' software [18].

The analysis of the XRD patterns reveals that all the samples exhibit single phase characteristics with no trace of other impurity phases (e.g., $Bi_2Fe_4O_9$, $Bi_{46}Fe_2O_{72}$, etc.). The rhombohedral distorted perovskite structure of $BiFeO_3$ with *R3c* space group is conserved as $xBa_{0.8}Sr_{0.2}TiO_3$ content increases up to $x = 0.3$ and at $x = 0.4$, it transforms into cubic structure (*Pm3m*). Fig. 1a and b shows the X-ray diffraction patterns of $(BiFeO_3)_{0.8}$–$(Ba_{0.8}Sr_{0.2}TiO_3)_{0.2}$ and $(BiFeO_3)_{0.6}$–$(Ba_{0.8}Sr_{0.2}TiO_3)_{0.4}$ ceramics respectively as examples. A similar phase transition from rhombohedral to cubic was observed at $x = 0.3$ for $(1-x)BiFeO_3$–$xBaTiO_3$ [9,10]. The structure and lattice parameters of different compositions in the system $(1-x)BiFeO_3$–$xBa_{0.8}Sr_{0.2}TiO_3$ are listed in Table 1. The lattice constant is not increasing monotonically with increase in *x*, but shows fluctuation. The ionic radii of $Ba^{2+}$ ($r(Ba^{2+}) = 1.36$ Å) and $Sr^{2+}$ ($r(Sr^{2+}) = 1.18$ Å) are larger then that of $Bi^{3+}$ ($r(Bi^{3+}) = 1.03$ Å), while the radius of $Ti^{4+}$ ($r(Ti^{4+}) = 0.605$ Å) is smaller than that of $Fe^{3+}$ ($r(Fe^{3+}) = 0.645$ Å) [19]. So

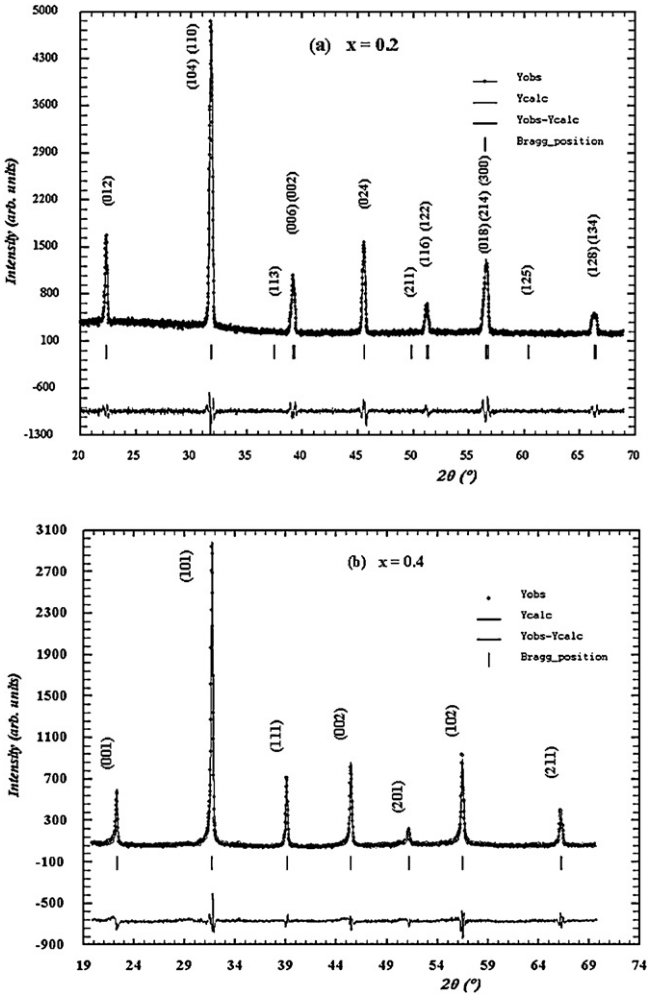


Fig. 1. XRD patterns for a rhombohedral and cubic ceramics samples of $(1-x)BiFeO_3$–$xBa_{0.8}Sr_{0.2}TiO_3$ with (a) $x = 0.2$ and (b) $x = 0.4$.

substitution of Ba and Sr in A site will result in an increase in crystal lattice constant while it is the reverse for the Ti substitution on site B. So, incorporation of $Ba_{0.8}Sr_{0.2}TiO_3$ is responsible for the fluctuation of the lattice constant.

The SEM micrographs of $(1-x)BiFeO_3$–$xBa_{0.8}Sr_{0.2}TiO_3$ samples with different compositions are shown in Fig. 2. Fig. 2a shows the surface of the specimen with composition $x = 0.1$. The microstructure was heterogeneous with bimodal grain size distribution, consisting of large grains of ∼8 μm and small grains of 3–4 μm. We can notice also that the substitution of $BiFeO_3$ by $Ba_{0.8}Sr_{0.2}TiO_3$ reduces the grain size and hence increases the volume fraction of grain boundaries and the

Table 1
Structure and lattice parameters of different compositions in the system $(1-x)BiFeO_3$–$xBa_{0.8}Sr_{0.2}TiO_3$.

| Composition $(1-x)BiFeO_3$–$xBa_{0.8}Sr_{0.2}TiO_3$ | Structure | Lattice parameters | |
|---|---|---|---|
| | | $a$ (Å) | $\alpha$ (°) |
| $x = 0.1$ | Rhombohedral | 5.638(2) | 59.382(6) |
| $x = 0.2$ | Rhombohedral | 5.620(6) | 60.157(1) |
| $x = 0.3$ | Rhombohedral | 5.619(7) | 60.159(4) |
| $x = 0.4$ | Cubic | 3.987(9) | – |

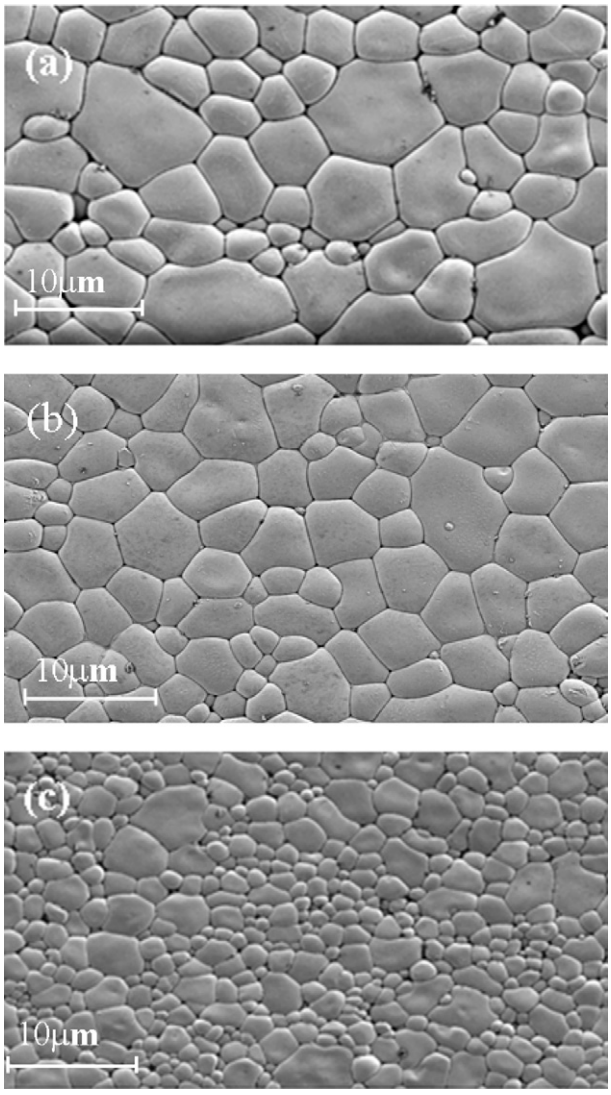


Fig. 2. Surface SEM images of the $(1-x)BiFeO_3$–$xBa_{0.8}Sr_{0.2}TiO_3$ ceramics: (a) $x = 0.1$, (b) $x = 0.2$ and (c) $x = 0.3$.

microstructure was relatively homogenous (Fig. 2b and c). With increasing $Ba_{0.8}Sr_{0.2}TiO_3$ content, the grain shapes become more regular, the grain sizes present a little decrease and the size distribution is more uniform.

### 3.2. Dielectric properties

The evolution of real parts ($\varepsilon'_r$) of the dielectric permittivity and dielectric loss (tan $\delta$) as a function of temperature at various frequencies of $(1-x)BiFeO_3$–$xBa_{0.8}Sr_{0.2}TiO_3$ ($x = 0$, 0.1, 0.2, 0.3, 0.4 and 1) samples is shown in Fig. 3. These dielectric measurements are reproducible after some thermal cycling from room temperature up to 600 °C.

For the composition $x = 0$ ($BiFeO_3$), the dielectric permittivity shows a continuously increase as the temperature increases. The measured values of the real part of permittivity are $\varepsilon'_r \approx 122$ at 300 °C and $\varepsilon'_r \approx 330$ at 400 °C at 100 kHz.

For all compositions in the range $0 < x \leq 1$, one anomaly of dielectric permittivity has been attributed to the ferroelectric–paraelectric transition temperature ($T_C$). These temperatures are about 496, 488, 478, 422 °C and 76 °C for $x = 0.1$, $x = 0.2$, $x = 0.3$, $x = 0.4$ and $x = 1$, respectively, at 100 kHz, decreasing as $x$ content increases. A similar behavior was observed by Kumar et al. [9,20] in $(1-x)BiFeO_3$–$xBaTiO_3$ system in which $T_C$ decreases from 504 to 372 °C for $x = 0.9$–0.7, respectively. However, the latter shows that for the composition $x = 0.4$, no dielectric anomaly is observed. This difference may be related to the introduction of $Sr^{2+}$ ion in A site in this new solid solution.

The maximum in dielectric permittivity observed at $T_C$ for 100 kHz in $(1-x)BiFeO_3$–$xBa_{0.8}Sr_{0.2}TiO_3$ system increases from 622 for $x = 0.1$, to 4565 for $x = 0.3$ and 6230 for $x = 0.4$, which are higher than that of $BiFeO_3$ (≈40 at room temperature) and smaller than that of $Ba_{0.8}Sr_{0.2}TiO_3$ (≈11,880) (Fig. 3). In $(1-x)BiFeO_3$–$xBaTiO_3$ system [9], the maximum in dielectric permittivity observed at $T_C$ for 100 kHz increases, less than our solution; from 300 for $x = 0.1$ to 4200 for $x = 0.3$. These results show that the dielectric performances of $BiFeO_3$ substituted by $Ba_{0.8}Sr_{0.2}TiO_3$ are better than with $BaTiO_3$.

The high value of the dielectric permittivity in $(1-x)BiFeO_3$–$xBa_{0.8}Sr_{0.2}TiO_3$ samples may be attributed to the conductivity thermally activated.

In addition, the maximum in dielectric permittivity observed at $T_C$ becomes broad as $x$ increases reflecting the diffuse characteristics of the phase transition which may be related to the structure disorder and compositional fluctuation produced in the arrangement of cations at A and B sites.The dielectric response exhibits frequency dispersion upon heating for all compositions. This dispersion decreases as $BiFeO_3$ content increases. So, this phenomenon can be explained by the random intrinsic barrier distribution [21].

The dielectric loss (tan $\delta$) of $BiFeO_3$ is about 0.02 at room temperature (Fig. 3) but it is of about 0.4 as observed by Wang et al. [15]. This difference can be explained by the difference in the preparation conditions. So the ceramic obtained in our case contains less porosity and inducing less conductivity in the material which is directly linked to tan $\delta$. As seen in Fig. 3, the dielectric loss (tan $\delta$) of all compositions shows a decrease with increasing frequency.

Above ∼300 °C, $(1-x)BiFeO_3$–$xBa_{0.8}Sr_{0.2}TiO_3$ ($x = 0.1$) shows steep upturns in tan $\delta$, with magnitude proportional to $1/f$, implying an existence of phase-shift conductivity due to random intrinsic barrier distribution of Bi and Ba and Sr ions on the A site, and Fe and Ti ions on the B site [15]. The origin of the increase of tan $\delta$ can be also due to the space charge polarization due to oxygen ions vacancies. A similar behavior of dielectric loss of $(1-x)BiFeO_3$–$xBaTiO_3$ system was observed [15]. Therefore, with the increase in $Ba_{0.8}Sr_{0.2}TiO_3$ content, dielectric permittivity of the system increases the transition temperature $T_C$ decrease and the dielectric loss tangents decreases.

### 3.3. Magnetic properties

Fig. 4 shows the room temperature magnetization hysteresis loops for $(1-x)BiFeO_3$–$xBa_{0.8}Sr_{0.2}TiO_3$ ($x = 0.1$, 0.2 and 0.3). In pure $BiFeO_3$, the magnetization varies linearly with the applied magnetic field up to 15 T. A similar magnetization character was also reported by other authors [22]. The magnetic

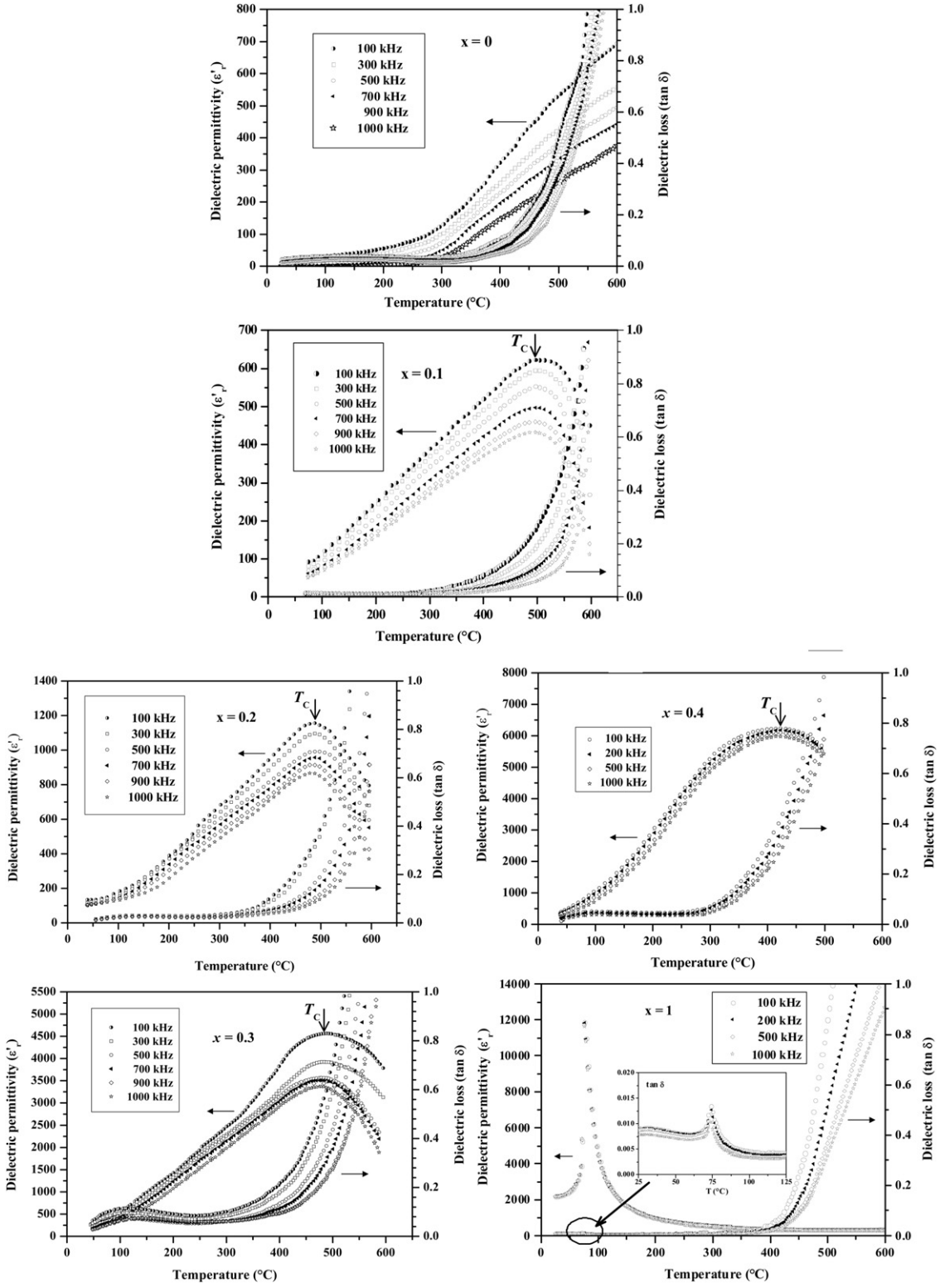


Fig. 3. Temperature dependence of the real part of the permittivity ($\varepsilon'_r$) and dielectric loss (tan $\delta$), for the compositions $x = 0$, $x = 0.1$, $x = 0.2$, $x = 0.3$, $x = 0.4$ and $x = 1$ upon heating.

structure of $BiFeO_3$ was proved to be antiferromagnetic with this G-type spin ordering below the Néel temperature [23,24]. However, the $Ba_{0.8}Sr_{0.2}TiO_3$ doped ceramics exhibited a magnetic hysteresis loops, referring to a quasi-ferromagnetic behavior. The magnetization curves were not really saturated even at 15 T, indicating the basic antiferromagnetic nature of the sample. Therefore, the appearance of hysteresis loops in our system may be attributed to the canting of antiferromagnetically ordered Fe–O–Fe chain of spins caused by the distortion created by non-magnetic ions Ti, Ba and Sr co-doping, resulting

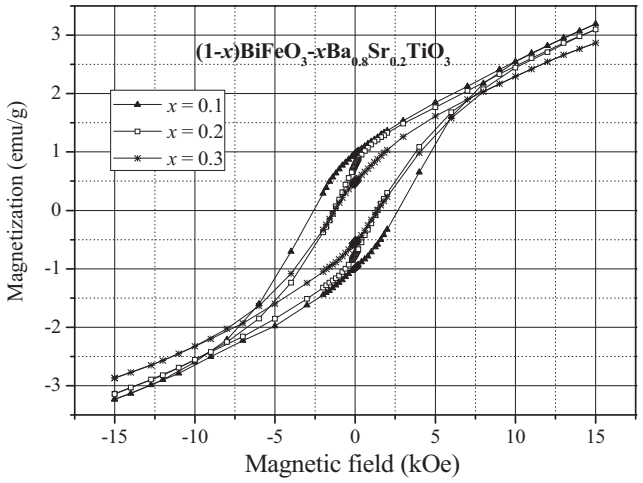


Fig. 4. Magnetic hysteresis loops for $(1-x)BiFeO_3$–$xBa_{0.8}Sr_{0.2}TiO_3$ ($0.1 \leq x \leq 0.3$) ceramics at room temperature.

in the weak spontaneous magnetic moment. An increasing magnetization was also reported by Itoh et al. [25] for small amounts of $BaTiO_3$ addition in $BiFeO_3$.

The remanent magnetization $M_r$ of the samples with $x = 0.1$, 0.2 and 0.3 are 0.971, 0.771 and 0.481 emu/g, and the coercive field $H_C$ of those samples are 2.616, 1.301 and 1.293 kOe, respectively. The highest remanent magnetization, coercive field and $M(H)$ loop area were found for the composition $x = 0.1$ and decrease as $Ba_{0.8}Sr_{0.2}TiO_3$ content increases. This behavior can be related, like dielectric properties, to grain size effect.

The $M_r$ of the $xBiFeO_3$–$(1-x)BaTiO_3$ samples with $x = 0.9$ and 0.8 are 0.313 and 0.383 emu/g, and the $H_C$ of those samples were 1.301 and 2.260 kOe, respectively at room temperature [10]. Compared to this study, the magnetic properties of $BiFeO_3$ are improved by introducing $Ba_{0.8}Sr_{0.2}TiO_3$.

## 4. Conclusion

In summary, a perovskite $(1-x)BiFeO_3$–$xBa_{0.8}Sr_{0.2}TiO_3$ ($x = 0$, 0.1, 0.2, 0.3, 0.4 and 1) ceramics were successfully prepared by the solid-state reaction method. The phase structure of the $(1-x)BiFeO_3$–$xBa_{0.8}Sr_{0.2}TiO_3$ ceramics changes from rhombohedral into cubic phase when the content of $Ba_{0.8}Sr_{0.2}TiO_3$ is in the range $0.3 \leq x \leq 0.4$. By comparison to $BiFeO_3$, our new compositions have high dielectric permittivity and low dielectric loss. Incorporation of $Ba_{0.8}Sr_{0.2}TiO_3$ in $BiFeO_3$ improves magnetic properties at room temperature. A remanent magnetization $M_r$ and a coercive magnetic field $H_C$ of about 0.771 emu/g and 1.301 kOe, respectively were obtained in specimen with composition $x = 0.2$ at room temperature.

## References

[1] M. Fiebig, T. Lottermoser, D. Frohlich, A.V. Goitsev, R.V. Pisarev, Observation of coupled magnetic and electric domains, Nature 419 (2002) 818–820.
[2] M. Fiebig, Revival of the magnetoelectric effect, Journal of Physics D 38 (2005) R123–R152.
[3] D.I. Khomskii, Multiferroics: different ways to combine magnetism and ferroelectricity, Journal of Magnetism and Magnetic Materials 306 (2006) 1.
[4] D. Ricinschi, K.Y. Yun, M. Okuyama, A mechanism for the 150 μC $cm^{-2}$ polarization of $BiFeO_3$ films based on first-principles calculations and new structural data, Journal of Physics: Condensed Matter 18 (2006) L97–L105.
[5] I. Sosnowska, T. Peterlin-Neumaier, E. Steichele, Spiral magnetic ordering in bismuth ferrite, Journal of Physics C: Solid State Physics 15 (1982) 4835–4846.
[6] G.A. Smolenskii, I. Chupis, Ferroelectromagnets, Soviet Physics Uspekhi 25 (1982) 475.
[7] C. Tabares-Munoz, J.-P. Rivera, A. Benzinges, A. Monnier, H. Schmid, Measurement of the quadratic magnetoelectric effect on single crystalline $BiFeO_3$, Japanese Journal of Applied Physics 24 (1985) 1051–1053.
[8] W.M. Zhu, Z.-G. Ye, Effects of chemical modification on the electrical properties of $0.67BiFeO_3$–$0.33PbTiO_3$ ferroelectric ceramics, Ceramics International 30 (2004) 1435–1442.
[9] M.M. Kumar, A. Srinivas, S.V. Suryanarayana, Structure property relations in $BiFeO_3$/$BaTiO_3$ solid solutions, Journal of Applied Physics 87 (2000) 855–862.
[10] F.P. Gheorghiu, A. Ianculescu, P. Postolache, N. Lupu, M. Dobromir, D. Luca, L. Mitoseriu, Preparation and properties of $(1-x)BiFeO_3$–$xBaTiO_3$ multiferroic ceramics, Journal of Alloys and Compounds 506 (2010) 862–867.
[11] T.-H. Wang, C.-S. Tu, H.-Y. Chen, Y. Ding, T.C. Lin, Y.-D. Yao, V.H. Schmidt, K.-T. Wu, Magnetoelectric coupling and phase transition in $BiFeO_3$ and $(BiFeO_3)_{0.95}$ $(BaTiO_3)_{0.05}$ ceramics, Journal of Applied Physics 109 (2011), 044101.
[12] I.P. Raevski, S.P. Kubrin, J.-L. Dellis, S.I. Raevskaya, D.A. Sarychev, V.G. Smotrakov, V.V. Eremkin, M.A. Seredkina, Studies of magnetic and ferroelectric phase transitions in $BiFeO_3$–$NaNbO_3$ solid solution ceramics, Ferroelectrics 371 (2008) 113–118.
[13] T.L. Ivanova, V.V. Gagulin, Dielectric properties in the microwave range of solid solutions in the $BiFeO_3$–$SrTiO_3$ system, Ferroelectrics 265 (2002) 241–246.
[14] Y.P. Wang, L. Zhou, M.F. Zhang, X.Y. Chen, J.M. Liu, Z.G. Liu, Room-temperature saturated ferroelectric polarization in $BiFeO_3$ ceramics synthesized by rapid liquid phase sintering, Applied Physics Letters 84 (2004) 1731.
[15] T.-H. Wang, C.-S. Tu, Y. Ding, T.-C. Lin, C.-S. Ku, W.-C. Yang, H.-H. Yu, K.-T. Wu, Y.-D. Yao, H.-Y. Lee, Phase transition and ferroelectric properties of $xBiFeO_3$–$(1-x)BaTiO_3$ ceramics, Current Applied Physics 11 (2011) S240.
[16] H. Abdelkefi, H. Khemakhem, G. Velu, J.C. Carru, R.V. Mubll, Dielectric properties and ferroelectric phase transitions in $Ba_xSr_{1-x}TiO_3$ solid solution, Journal of Alloys and Compounds 399 (2005) 1–6.
[17] W.J. Merz, The electric and optical behavior of $BaTiO_3$, single-domain crystals, Phys. Rev. 76 (1949), 212102.
[18] J. Rodriguez-Carvajal, Program Fullprof, Laboratoire Léon Brillouin, CEA-CNRS, version Avril 2008, LLB-LCSIM, 2008.
[19] R.D. Shannon, Revised effective ionic radii and systematic studies of interatomic distances in halides and chalcogenides, Acta Crystallographica. Section A, Crystal Physics, Diffraction, Theoretical and General Crystallography 32 (1976) 751–767.
[20] M. Kumar, K.L. Yadav, The effect of Ti substitution on magnetoelectric coupling at room temperature in the $BiFe_{1-x}Ti_xO_3$ system, Journal of Physics: Condensed Matter 18 (2006) L503–L508.
[21] V.H. Schmidt, G.F. Tuthill, C.S. Tu, T.V. Schogoleva, S.C.M. Eschia, Random barrier height model for phase shifted conductivity in perovskites, Ferroelectrics 199 (1997) 51–57.
[22] V.R. Palkar, D.C. Kundaliya, S.K. Malik, S. Bhattacharya, Magnetoelectricity at room temperature in the $Bi_{0.9-x}Tb_xLa_{0.1}FeO_3$, Physical Review B 69 (2004), 212102.
[23] I. Sosnowska, A.K. Zvezdin, Origin of the long period magnetic in $BiFeO_3$, Journal of Magnetism and Magnetic Materials 140 (1995) 167–168.
[24] B. Ruette, S. Zvyagin, A.P. Pyatakov, A. Bush, J.F. Li, V.I. Belotelov, A.K. Zvezdin, D. Viehland, Cycloidal to homogeneous spin order magnetic-field-induced phase transition in $BiFeO_3$ observed by high-field electron spin resonance, Physical Review B 69 (2004), 064114.
[25] N. Itoh, T. Shimura, W. Sakamoto, T. Yogo, Fabrication, Fabrication and characterization of $BiFeO_3$–$BaTiO_3$ ceramics by solid state reaction, Ferroelectrics 356 (2007) 19–23.